



# NIH Public Access

## Author Manuscript

Biochemistry. Author manuscript; available in PMC 2014 November 19.

Published in final edited form as:  
*Biochemistry*. 2013 November 19; 52(46): 8342–8351. doi:10.1021/bi401303v.

## Some Ligands Enhance the Efflux of Other Ligands by the *Escherichia coli* Multidrug Pump AcrB

Alfred D. Kinana<sup>†</sup>, Attilio V. Vargiu<sup>‡</sup>, and Hiroshi Nikaido<sup>†,\*</sup>

<sup>†</sup>Department of Molecular and Cell Biology, University of California, Berkeley California 94720

<sup>‡</sup>Department of Physics, University of Cagliari, S.P. 8 km 0.700, Monserrato (CA), 09042 Italy

### Abstract

By measuring quantitatively the active efflux of cephalosporins by an RND (resistance-nodulation-division) family efflux pump AcrB in intact cells of *Escherichia coli*, we found that the simultaneous presence of another substrate, such as chloramphenicol, benzene, cyclohexane, or Arg β-naphthilamide significantly enhanced the extrusion of cephalosporins. The stimulation occurred also in a strain expressing the covalently linked trimer of AcrB, and thus cannot be ascribed to the enhanced assembly of the trimer from AcrB monomers. When Val139 of AcrB was changed into Phe, the stimulation by benzene was found to occur at much lower concentration of the solvent. A plausible explanation of these observations is that the AcrB pump is constructed to pump out very rapidly the solvent or chloramphenicol molecules, and thus the efflux of cephalosporins, which presumably bind to a different subsite within the large binding pocket of AcrB, can become facilitated. Computer simulations of ligand binding to AcrB, both by docking and by molecular dynamics simulations, produced results supporting and extending this hypothesis. Benzene and the cephalosporin nitrocefin can bind simultaneously to the distal binding pocket of AcrB, both in the wild type and in the V139F variant. Interestingly, while the binding position and strength of benzene are almost unaffected by the presence of nitrocefin, this latter substrate is significantly displaced towards the exit gate in both wild type and mutant transporter in the presence of benzene. Additionally, the cephalosporin efflux may be enhanced by the binding of solvents (sometimes to the cephalosporin-free protomer) which could accelerate AcrB conformational changes necessary for substrate extrusion.

### Keywords

multidrug efflux; solvents; cephalosporins; chloramphenicol; positive cooperativity

### Introduction

RND (Resistance-Nodulation-Division) family transporters<sup>1</sup>, such as AcrB of *Escherichia coli*, pump out drug molecules mostly from the periplasm of Gram-negative bacteria directly into the external medium, through collaboration with an outer membrane channel (TolC in the case of AcrB) and a periplasmic accessory protein (AcrA in the case of AcrB)<sup>2</sup>. Some of these transporters, including AcrB, handle a very wide range of ligands, including antibiotics, biocides, dyes, detergents<sup>3</sup>, and even simple solvents<sup>4, 5</sup>. In our previous attempt to predict the binding of these ligands to the deep binding pocket of the AcrB protein<sup>6</sup>, we

\*Department of Molecular and Cell Biology, Room 426 Barker Hall, University of California Berkeley, Berkeley, CA 94720-3202, USA; Phone 510-642-2027; nhiroshi@berkeley.edu.

**Supporting Information Available.** Details of Experimental Procedures and additional Figures are presented. This material is available free of charge via the Internet at <http://pubs.acs.org>.

used computer prediction algorithm of Autodock Vina and found that some ligands, including nitrocefin, bind to the narrow “groove” of the pocket whereas others, including chloramphenicol and benzene, bound to a much wider “cave” area of this large pocket. We examined whether the simultaneous presence of two ligands results in competition. As we can measure the efflux of nitrocefin in a quantitative, real-time assay<sup>7</sup>, this was followed in the presence of minocycline, a groove-binder, and of chloramphenicol, a cave-binder. The results showed that minocycline strongly inhibited the efflux of nitrocefin presumably by interfering with the binding of the latter to the groove, whereas there was no evidence of inhibition when chloramphenicol was added<sup>6</sup>.

Examination of chloramphenicol data suggested in addition that the drug, especially at higher concentrations, actually may enhance, rather than inhibit, the efflux of nitrocefin. Because such mutual stimulation between ligands, if true, may shed light into the mechanism of efflux transport, we began by confirming the reproducibility of these data. We then found that other ligands, especially solvents such as benzene and cyclohexane, which are substrates of the AcrB pump<sup>4, 5</sup>, strongly accelerated the efflux of nitrocefin and another cephalosporin, cefamandole. We examined the binding of both nitrocefin and benzene to AcrB both by computer docking and by molecular dynamics simulation, and discuss possible mechanisms of this stimulation phenomenon.

## EXPERIMENTAL PROCEDURES

### Bacterial strains

For the measurement of cephalosporin efflux, *E. coli* K12 strains HN1157 and HN1160<sup>7</sup> were used for nitrocefin and cefamandole, respectively. In both of these strains, the expression of the AcrAB efflux pump was increased by the deletion of the *acrR* repressor gene. HN1157 also contained a mutated porin gene producing a larger pore channel, so that the influx of nitrocefin across the outer membrane was facilitated. In HN1160, the endogenous AmpC  $\beta$ -lactamase, with low  $K_M$  values for cephalosporins, was replaced by the TEM  $\beta$ -lactamase with much higher  $K_M$  values.

### Culture of strains and nitrocefin efflux assay in the presence and absence of other substrates

Strains were grown in M63 medium ((NH<sub>4</sub>)<sub>2</sub>SO<sub>4</sub> 15 mM; MgSO<sub>4</sub> 1 mM; FeSO<sub>4</sub> 1.3  $\mu$ M; 0.1 M K-phosphate buffer at pH 7.0; 0.2% glucose) at 30°C with shaking until the cell culture reached an OD<sub>600</sub> of 0.65. For the growth of HN1160, arginine (20  $\mu$ g/ml) and thiamine (1  $\mu$ g/ml) were added to this medium. Cells were harvested by centrifugation, washed twice and re-suspended in 50mM potassium phosphate buffer, pH 7.0 containing 5mM MgCl<sub>2</sub> to a final OD<sub>600</sub> of 0.8. Samples were split into two sets of cuvettes. In one set, a stimulator substrate was added to a specified final concentration. In the other set, no substrate was added. Samples were pre-incubated at room temperature for 5 to 10 min. Nitrocefin or cefamandole was then added, and efflux assays were performed as described previously<sup>7</sup>.

### Construction of an *acrB* mutant and gene replacement in *E. coli* genome

First, the wild type sequence of *acrB* from HN1157<sup>7</sup> was amplified by PCR and cloned into pSPORT1 vector between BamHI and SmaI restriction sites. The mutation V139F was introduced by site-directed mutagenesis using pfu Ultra High fidelity DNA polymerase (Agilent) as described by the manufacturer. The mutant gene was then subcloned into pKO3 vector<sup>8</sup> between BamHI and SmaI restriction sites, giving pKO3/*acrB*\_V139F plasmid. This plasmid was electroporated into HN1157, the chromosomal integrates were selected at 42°C, and the strains that lost the vector sequence was selected with 5% sucrose<sup>8</sup>, resulting in the strains in which the *acrB* gene was replaced with the mutant gene coding for the V139F

sequence. Gene replacement was confirmed by PCR using a forward primer annealing on *acrA* and a reverse primer annealing on *acrB*, followed by DNA sequencing. The oligonucleotide primers used for PCR amplification and site-directed mutagenesis are shown in Table 1 of the Supporting Material.

### Determination of minimal inhibitory concentration (MIC)

MIC of nitrocefin was determined in the presence and absence of 32 µg/ml Arg β-naphthylamine, by streaking a culture of HN1157 on an LB plate containing a linear gradient of nitrocefin (0 to 25 µg/ml) and by incubating the plate overnight at 37 °C.

### Docking and MD simulations

**Docking**—In the bi-molecular complexes the starting position of each substrate within the distal pocket of the Binding protomer (for MD simulation) was taken either from our previous study<sup>9</sup> or from docking calculations performed with the AUTODOCK VINA package<sup>10</sup> using as a target the crystal structure of AcrB<sup>11</sup> (wt protein) and that resulting from structural relaxation of mutant AcrB free of substrates (V139F variant). The latter model was constructed by introducing the V139F mutation in the Binding Protomer of the AcrB model 2J8S<sup>11</sup> through the mutator plugin of VMD<sup>12</sup>, following the procedure described earlier<sup>13</sup>. After preliminary energy minimization by this program, the structure was optimized by MD simulation.

In the tri-molecular complexes, the second ligand was docked on the two top conformations extracted from the MD simulation of bi-molecular complexes, by a cluster analysis performed on the equilibrium trajectories. Further details are described in Supporting Information.

**MD simulations**—The setup for the MD simulations of bi- and tri-molecular complexes was identical to that reported previously<sup>9</sup>. A reduced model of the protein was used, only including the periplasmic loops responsible for the substrate specificity of AcrB<sup>14</sup>. Further details and calculation of binding energy through MM/GBSA approach and metadynamics are described in Supporting Information.

## RESULTS

### Nitrocefin efflux is stimulated by chloramphenicol

In our previous study comparing the effects of minocycline and chloramphenicol on the efflux of nitrocefin<sup>6</sup>, we noted that the former acted as a powerful inhibitor whereas the latter showed no visible inhibition. A careful examination of these data showed that there was a slight stimulation of nitrocefin efflux in the presence of chloramphenicol, however at that time only efflux rates at different external concentrations of nitrocefin were compared. To confirm that the stimulation was real, a more thorough analysis was performed in which we examined the precise kinetics of efflux, by plotting the efflux rates at different nitrocefin concentrations in the periplasm, where its capture takes place<sup>7</sup>. Such an analysis (Fig. 1) showed that the stimulation was slight but real, mainly resulting from approximately 20% increase in  $V_{max}$  and possibly also from a decrease in  $K_M$  (less than 10%).

### Nitrocefin efflux is stimulated by solvents

We tried to find other AcrB substrates that stimulated the efflux of nitrocefin more strongly, so that further analysis would become facilitated. High concentrations (30 mM) of both benzene and cyclohexane produced strong stimulation of nitrocefin efflux (Fig. 2A and 2B). Similarly, 25 mM cyclohexanone produced a remarkable activation of nitrocefin flux (Fig.

2C). We examined the possibility that the solvents might be directly interfering with the hydrolysis of nitrocefin catalyzed by the AmpC  $\beta$ -lactamase. However, the solvents had no effect on nitrocefin hydrolysis by the sonicated cell extracts. At these high concentrations, solvents caused increases in the  $V_{max}$  values, and often decreased the values of  $K_M$ ; for example, in two experiments with benzene,  $V_{max}$  was increased about twofold, and  $K_M$  was decreased also twofold (not shown).

Although these results were encouraging, solvents were used at concentrations much higher than that of the measured efflux substrate, nitrocefin. At such concentrations we cannot exclude the possibility that solvent effect was caused by their strong partition into the bilayer, which may affect the function of the transporter. (However, this mechanism is unlikely in the V139F mutant AcrB described below). At concentrations comparable to the nitrocefin concentration, i.e. around 0.1 mM, the effect was more modest, although a clear indication of stimulation was seen (see below). We have tested a number of other potential substrates of the AcrB pump at 0.1 mM concentration. We could not find any evidence of stimulation of nitrocefin efflux in the presence of the following substrates: deoxycholate, taurocholate, novobiocin, erythromycin, azithromycin, ciprofloxacin, norfloxacin, and nalidixic acid (results not shown).

### Nitrocefin efflux is stimulated by Arg $\beta$ -naphthylamide

The well-known AcrB inhibitor (and substrate<sup>15</sup>) Phe-Arg  $\beta$ -naphthylamide inhibited nitrocefin efflux when used at a low concentration (20  $\mu$ M), but at a higher concentration (0.1 mM) it often produced stimulation (results not shown). Although this compound was recently reported to increase the non-specific permeability of the outer membrane<sup>16, 17</sup>, such an effect at high concentrations was known already at the time of its discovery<sup>15</sup> and its activity as an efflux inhibitor is supported by a large number of studies<sup>18</sup>. Because Phe-Arg  $\beta$ -naphthylamide is hydrolyzed by intact *E. coli* cells first into Phe and Arg  $\beta$ -naphthylamide by peptidase N (T. May and H. Nikaido, unpublished), Arg  $\beta$ -naphthylamide was tested and indeed found to be a powerful stimulant of nitrocefin efflux (Fig. 3). A large decrease in the values of  $K_M$  ( $81 \pm 6.3\%$  decrease in four experiments) played a major part here, although there was also a modest increase in  $V_{max}$  in all experiments. Neither Phe nor the further hydrolysis product of Arg  $\beta$ -naphthylamide, Arg and  $\beta$ -naphthylamine, produced significant stimulation (or inhibition).

When nitrocefin MIC was determined by using the gradient plate method in the presence of 32  $\mu$ g/ml (0.107 mM) Arg  $\beta$ -naphthylamide, there was a slight but reproducible increase in MIC, from 11.1 to 13.1  $\mu$ g/ml, consistent with the stimulation of nitrocefin efflux (Fig. S1). Although the increase was smaller than expected, this could be due to the instability of the stimulator, Arg  $\beta$ -naphthylamide, which is hydrolyzed by peptidase N.

### Efflux of cefamandole is also stimulated by solvents and chloramphenicol

Nitrocefin binds very tightly to the distal binding pocket of AcrB<sup>9</sup>, and its transport  $K_M$  is by far the lowest among the cephalosporins tested<sup>7</sup>. In order to show that the stimulation phenomenon is not solely limited to this tight-binding substrate, we used cefamandole, which is expected to bind less tightly than nitrocefin to the binding site, with the calculated binding energy (in docking with Autodock Vina) of -9.2 kcal/mol in contrast to that of -10.2 kcal/mol for nitrocefin. Indeed, cefamandole is pumped out by AcrB with a much higher  $K_{0.5}$  value of around 20  $\mu$ M than the  $K_M$  of nitrocefin (around 5  $\mu$ M)<sup>7</sup>. Cefamandole efflux was indeed stimulated by 0.1 mM and 30 mM benzene (Fig. 4A and B) reproducibly. Chloramphenicol (0.1 mM) also produced a significant stimulation of cefamandole efflux (Fig. 4C). The efflux kinetics of cefamandole shows a strong cooperativity<sup>7</sup>, and thus its analysis becomes more complicated. However, the stimulation again seems to be caused

mainly by increases in  $V_{max}$  and decreases in  $K_{0.5}$ . Interestingly, in all experiments there appeared to be a significant decrease in apparent cooperativity, the calculated Hill coefficients decreasing to 63, 81, 81, and 91% of the no-solvent control value (average 2.69) in the four experiments with 30 mM benzene.

### Stimulation of nitrocefin efflux is not caused by the accelerated assembly of AcrB trimer

According to the functionally rotating trimer concept of AcrB function, AcrB cannot perform its efflux function unless it is assembled into a homotrimer. Thus it is possible that solvents stimulate the efflux by somehow facilitating the assembly of the AcrB trimer. This was tested by using the covalently linked, giant AcrB trimer produced from the modified gene coding for such a complex<sup>19</sup>. The stimulatory effect of benzene was indeed confirmed in the linked trimer (Fig. 5)

### Studies with the V139F mutant AcrB

The results presented above suggested that the effect of stimulants (such as solvents) is likely to involve the interaction (either direct or allosteric) of these ligands and cephalosporins in an AcrB trimer. In an effort to understand how this interaction could occur within the large (distal) binding pocket of AcrB, docking prediction was made with Autodock Vina. The calculated binding energy of benzene to the AcrB binding pocket was quite small ( $-5.1$  kcal/mol), and it appeared to bind to the lower (i.e. closer to the membrane surface) part of the binding pocket, earlier called “cave”<sup>6</sup>, at a location closest to the Val139 residue (with the closest distance of  $3.2$  Å) (Fig. 6). We thus tried to strengthen the binding of benzene to this region of the binding pocket by mutating Val139 to a Phe residue. This mutation was constructed and the wild-type *acrB* gene was replaced by this mutant gene as described in Experimental Procedures.

When nitrocefin efflux was measured in this mutant, a much stronger stimulation by 0.1 mM benzene was observed (Fig. 7B), in comparison with the cells producing the wild type AcrB (Fig. 7A). In the mutant, stimulation was apparently caused by an increase (about 60%) in  $V_{max}$ , and a strong decrease (by about 60%) in  $K_M$ . It was stimulated less strongly by the presence of 0.1 mM cyclohexane, however (Table 1).

### Docking studies

In an effort to understand the mechanism of stimulation of nitrocefin and cefamandole efflux by various ligands, we examined the binding of the substrates and stimulators to the distal binding pocket of the binding protomer of AcrB with Autodock Vina. Initially, we focused on benzene and nitrocefin, which were predicted to bind to two distinct sub-areas of the binding pocket. Benzene was predicted to bind to the lower part of the pocket, previously named “cave”<sup>6</sup>, with a low affinity ( $-5.1$  kcal). Nitrocefin, which is predicted to bind very tightly to the pocket of the free AcrB (with the calculated energy of  $-10.2$  kcal), was found to bind less tightly to AcrB with a pre-bound benzene ( $-9.4$  kcal) as the thiophene ring of nitrocefin clashes with the benzene, and was thus displaced by this molecule. As for cefamandole, it is predicted to bind somewhat less tightly ( $-9.2$  kcal) than nitrocefin, exclusively to the upper, “groove” region of the pocket<sup>6</sup>, and thus will be less affected by the binding of benzene to the lower region of the pocket. However, Autodock Vina predicts that Arg β-naphthylamide binds tightly ( $-9.9$  kcal) to the subdomain that is also occupied by nitrocefin, and the effort to dock nitrocefin to AcrB with the pre-bound Arg β-naphthylamide ended up with the prediction that nitrocefin will preferentially bind to sites that are completely outside of the pocket.

Similar docking studies were carried out with an MD-simulation-optimized model of V139F mutant AcrB. Compared with the wild-type AcrB, benzene was indeed found to bind with a higher affinity ( $-8.5$  kcal), and nitrocefin with a lower affinity ( $-8.6$  kcal).

## MD simulation studies

Because docking cannot take into account the effect of water molecules and the substrate-induced changes in the conformation of the binding site, we examined some of these interactions by MD simulations, concentrating on nitrocefin and benzene (Table S1).

**(i) Benzene alone**—We started from the most stable docked structures of the benzene-(wild type)AcrB complex (Fig. 8A). In one simulation, benzene kept hopping between two different positions in the binding site (Fig. 8B–C and Figs. S2 and S3). Calculated binding free energies were similar at these two positions (Table 2). In another simulation, starting from a different but energy-equivalent binding pose, benzene remained essentially in the same, lower part of the binding pocket (Figs. 8D). In all the poses, benzene tended to be loosely surrounded by several hydrophobic residues, including the aromatic F136, F178, Y327, V571, F610, and F628 (Table S2).

In the V139F AcrB, the initial docked position showed benzene indeed interacting more tightly (see above) with the phenyl group of the newly created F139 with a loose stacking interaction at the distance of about  $4\text{ \AA}$  (Fig. 8E). At the end of MD simulations, the binding site has undergone significant changes of conformation, and in two independent MD simulations the benzene molecule became sandwiched between the F139 and F628 (Figs. 8F–G), although its binding position did not change dramatically with respect to that in wild type AcrB (Fig. S3). Also the key residues stabilizing benzene within the pocket were well-conserved compared to the complex with the unaltered AcrB (Table S2).

In the MD simulations, benzene seemed to bind more stably to the V139F variant of AcrB (Fig S3A), yet the MM/GBSA approach was unable to reflect this feature in the values of the binding free energy (see Table 2), possibly because the entropy term was not included<sup>9</sup>. We therefore used a more powerful approach, metadynamics<sup>20–23</sup> (see Experimental Procedure in Supporting Information) in order to evaluate the free energy cost associated with the displacement of benzene from the Phe-rich cage. This quantity can be related to the residence time of benzene in the binding pocket, which in turn might be inversely related to the rate at which AcrB conformational changes occur along the functional rotation cycles (see Discussion). We chose a simple and intuitive collective variable (CV) to be biased, i.e. the distance between the centers of mass of benzene and of residues surrounding it (see Supporting Information). The affinity of benzene was indeed higher for the mutated than for the wild type protein. Namely, the packing of the solvent by residues F136 and F139 increases by  $\sim 3$  kcal/mol the free energy barrier associated to unbinding from the most stable position in the pocket (Fig. S4). In addition to the well-tempered metadynamics simulations, we performed an additional set of standard metadynamics simulations, without any wall on the distance between benzene and the center of mass of the pocket. Interestingly, in three different simulations performed for each system, benzene exited the protein from the external cleft in the wild type complex, and reached the exit gate in the mutated protein (data not shown). This surprising finding, however, is consistent with a larger stimulation, by benzene, of nitrocefin efflux in the V139F variant (Fig. 7B).

**(ii) Nitrocefin alone**—We extended to 165 ns the simulation of the nitrocefin-(wild type)AcrB reported earlier<sup>9</sup> (Table S1), but there were no significant changes in the binding position and affinity (Figs. 9A–B and Table 2). When docking of nitrocefin was carried out with AcrBV139F, the binding was weaker than with the wild type AcrB, as described above.

One of the few prominent interaction was the loose (~4 Å) sandwiching of the thiophene ring of nitrocefin between F139 and F628 (Fig. 9C). In the subsequent MD simulation nitrocefin contacts with the protein and water were optimized, and the thiophene ring lost contacts with F139 (Fig. 9D).

**(iii) Nitrocefin binding to benzene-AcrB complex**—We investigated how nitrocefin binding is affected by the presence of a benzene molecule in AcrB. When docking of nitrocefin was carried out using representative benzene-AcrB(wild type) conformations optimized by MD simulations, we found that it bound less tightly to the transporter: the binding energy calculated by Vina (obtained by empirical methods, and cannot be compared to the free energies in Table 2) were in the range of -8.0 to -9.1 kcal/mol, weaker than the -10.2 kcal/mol energy obtained for wild type AcrB free of benzene. Two opposite orientations of nitrocefin were found to be compatible with pre-bound benzene in the distal pocket (data not shown). The difference in affinity compared to the bimolecular complex was retained in the binding free energy calculated over the two MD trajectories (one per orientation of nitrocefin) of the trimolecular system nitrocefin-benzene-AcrB (Table 2).

Interestingly, compared with the bimolecular complexes, in one of the MD simulations benzene moved by a few Å towards the upper part of the distal pocket (Fig 10A), and the pattern of stabilizing contacts was only partly conserved (Table S2). In both wild type and mutant tri-molecular complexes, nitrocefin moved more significantly in the direction of the Exit Gate towards the TolC docking domain<sup>11</sup>, with the carboxyl group facing residues Q124 and Y758 (compare the stick models of nitrocefin in green and lime with those in red and mauve in Fig. 10B). This movement of the substrate was also seen in the second MD simulation started from a different conformation of the benzene-AcrB complex (where nitrocefin assumed a flipped orientation with respect to the first simulation, see Figs. S5A and S5C), although its magnitude was somewhat less (Table S1). In this case the axis of nitrocefin was not fully aligned to the Binding Pocket-Gate direction. Several key interactions with residues of the binding pocket were retained despite this displacement (Table S3), although the overall interaction strength was reduced (Table 2). MD simulations thus showed that the two substrates can bind simultaneously to the distal pocket, benzene in the bottom and nitrocefin (in two opposite orientations) in the upper part, closer to the Exit Gate.

## DISCUSSION

We detected some hints earlier<sup>6</sup> that the presence of one ligand, chloramphenicol, may enhance the efflux of another ligand, nitrocefin, added at the same time. The differences were small, yet this conclusion could be confirmed in the present study (Fig. 1). We further showed in this study that, when tested at high concentrations (around 30 mM), simple solvents such as benzene, cyclohexane, and cyclohexanone stimulated much more strongly the efflux of nitrocefin, partly by increasing its  $V_{max}$  for transport (Fig. 2). Other than the solvents, Arg β-naphthylamide stimulated nitrocefin efflux strongly (Fig. 3). In a mutant AcrB (V139F), benzene could produce a strong stimulation of nitrocefin efflux even at a low concentration of 0.1 mM (Fig. 7B). Finally, benzene and chloramphenicol produced a modest but reproducible stimulation of the efflux of cefamandole (Fig. 4), another cephalosporin.

Stimulation, by one substrate, of the efflux of another substrate is not unknown in the behavior of multidrug transporters. It is well-known that the transport of Hoechst 33342 dye by the P-glycoprotein is stimulated by the simultaneous presence of another substrate, rhodamine 123<sup>24, 25</sup>, an observation that led to the assumption that there are two distinct substrate binding sites (H-site and R-site for the Hoechst dye and rhodamine, respectively)

NIH-PA Author Manuscript NIH-PA Author Manuscript NIH-PA Author Manuscript

that are separated by a measurable distance<sup>26</sup>. Since P-glycoprotein functions as a monomer, such stimulation phenomena likely involve allosteric conformational changes introduced by the binding of one of the substrates<sup>27</sup>. In contrast, AcrB operates as a trimer, and the binding and export of substrates presumably involves tight interaction between the neighboring protomers<sup>11,28,29</sup>; thus the mechanism of stimulation may be more complex.

One trivial mechanism involves the accelerated assembly of AcrB trimer by the stimulator substrate, but we were able to show that this mechanism cannot explain our observations, because even covalently linked trimeric AcrB was stimulated by benzene (Fig. 5). (However, at present we cannot rule out the possibility that the assembly of the AcrB-AcrA-TolC tripartite complex might be affected.) In the next step, we considered the interaction between the substrates within a single AcrB protomer, by examining the binding of substrates to the distal binding pocket of AcrB, which plays a critical role in the export process<sup>29, 30</sup>. Computational docking suggested that the initial binding of benzene to the “lower” part of this pocket weakens the subsequent binding of nitrocefin, mainly to the “upper” part of the pocket, a conclusion supported by the MD simulation, showing 5 to 6 kcal/mol decrease in the absolute value of the binding energy of nitrocefin when benzene was simultaneously present in the pocket (Table 2). Since nitrocefin appears to bind to the pocket of AcrB exceptionally tightly, as judged by its very low transport  $K_M$  value<sup>7</sup> and its large calculated binding energy (see Table 2 of our previous paper<sup>9</sup>), it seemed possible, *a priori*, that a weakened binding of this substrate may explain its increased efflux by the minimization of the energy trough of binding. However, there are several lines of evidence against this hypothesis. First, the efflux of cefamandole, which appears to bind to the pocket much more loosely than nitrocefin on the basis of its higher transport  $K_M$  (actually  $K_{0.5}$ )<sup>7</sup> and the smaller binding energy than nitrocefin (see Results), is nevertheless stimulated by the presence of benzene (Fig. 4). Second, in the strain expressing the V139F mutant AcrB, benzene causes hardly a decrease in the binding energy of nitrocefin (Table 2), although benzene strongly stimulates nitrocefin efflux (Fig. 7). Third, it is difficult to explain, by this hypothesis, the strong stimulation of nitrocefin efflux caused by Arg β-naphthylamide, because both substrates are expected to bind to a similar area of the pocket.

In fact, MD simulations gave us some hints that may at least partially explain the efflux stimulation data. When nitrocefin was present together with benzene in the binding site, the former was eventually pushed for about 7 Å toward the exit gate (Fig. 10B), suggesting that the presence of benzene could favor the accelerated efflux of nitrocefin. In addition, more than one molecule of small substrates, such as benzene, may bind to the same binding pocket at the same time, and this could produce stimulation of efflux.

An important factor we have not considered may be the binding of substrates in successive binding pockets in the same AcrB protomer, or in different protomers within the trimeric assembly. Thus the existence of a more proximal binding pockets, earlier identified in the symmetric AcrB crystals<sup>31–34</sup> and by Cys mutagenesis studies<sup>30</sup>, was now confirmed to be present in the Access protomer by crystallography involving asymmetric crystals<sup>35, 36</sup>. The extrusion of a drug molecule bound in the Binding protomer thus would either require, or be at least stimulated by, the binding of the next drug molecule to the proximal binding site of the neighboring Access protomer. It seems likely that the “stimulating” substrate, such as solvents or Arg β-naphthylamide, could affect the efflux of the measured substrate, such as nitrocefin or cefamandole bound in the Binding protomer, in this manner. The stimulation by Arg β-naphthylamide, a large compound that is predicted to bind to the same area in the distal binding pocket as nitrocefin, seems to require such a mechanism. Such interaction between the neighboring protomers was indeed the mechanism proposed to explain the positive cooperativity in the efflux of various cephalosporins<sup>7</sup> and penicillins<sup>37</sup>. If this is the case, the efflux of cefamandole is limited by the rate at which the neighboring Access

protomer would bind the next cefamandole molecule when it is the only substrate present. Since solvent molecules are predicted to enter (and exit) the AcrB binding pockets rapidly, as discussed below, the cefamandole efflux is likely accelerated by the rapid entry of solvents (and other substrates that are pumped out rapidly) into the neighboring Access protomer, when these substrates are also present. Cefamandole and solvent molecules could also bind to the same protomer, and could be extruded simultaneously. We indeed found that benzene decreased the Hill coefficient for the efflux of cefamandole, an observation that supports our hypothesis.

It is well-known that AcrB pumps out solvents<sup>5</sup>. Importantly this efflux seems to occur with very high turnover numbers. Although the kinetic constants of benzene efflux through AcrB are not known, we can make a rough estimate as follows. The permeability coefficient of benzene in a conventional phospholipid bilayer was estimated as 9.9 cm/s by MD simulations<sup>38</sup>. Assuming that outer membrane bilayer has permeability about three orders of magnitude lower than the conventional bilayer<sup>39</sup>, we can estimate the permeability coefficient of benzene here as 0.01 cm/s. Thus if AcrB decreases the periplasmic benzene concentration by 10% when the cells are exposed to 100  $\mu$ M benzene, creating a 10  $\mu$ M concentration gradient across the outer membrane, benzene will diffuse into the periplasm at a rate of 13.2 nmol/mg cells/s. To counteract this influx, AcrB must pump out the solvent at about this rate. This can be compared with the low  $V_{max}$  values for the efflux of nitrocefin and cefamandole (0.02 and 0.4 nmol/mg cells/s, respectively)<sup>7</sup>. Similarly, although the efflux rate of chloramphenicol is not known, we can assume that it is rapid, as it must penetrate across the outer membrane, mainly through the porin channels, rapidly as it is relatively small and uncharged<sup>40</sup>. These considerations suggest that the stimulators of cephalosporin efflux in AcrB are likely to be compounds that are very rapidly pumped out as substrates.

In general, it is difficult to know the rate-limiting steps in a secondary transporter. However, in one case that has been studied extensively, LacY of *E. coli*, it appears to be the rate of conformational alteration generating the outward-open conformer, rather than the rate of substrate binding<sup>41</sup>. Perhaps in AcrB also, it seems possible that various substrates facilitate, to a different degree, the large conformational change from the Binding to Extrusion conformation<sup>11, 28, 29</sup> necessary for the drug export. Finally it is also possible that stimulator substrates enter rapidly into the deep binding pocket without being trapped in the proximal binding pocket<sup>42</sup>, thereby producing an accelerated functional cycle through which the efflux of other larger substrates becomes accelerated.

## Supplementary Material

Refer to Web version on PubMed Central for supplementary material.

## Acknowledgments

A. V. V. thanks Paolo Ruggerone for useful discussions and continuous support. The authors acknowledge gratefully computational resources from the Lawrence Berkeley National Laboratory (Berkeley, CA) and from CINECA (Bologna, Italy; PRACE 4th Call grant "Understanding the bacterial efflux systems: insights into structure-function relationship from all-atom simulations" and ISCRA-A Grant HP10ARSZ26).

## Funding Sources

This study was supported in part by a grant from U.S. Public Health Service AI-009644 (to H. N.).

## Abbreviations

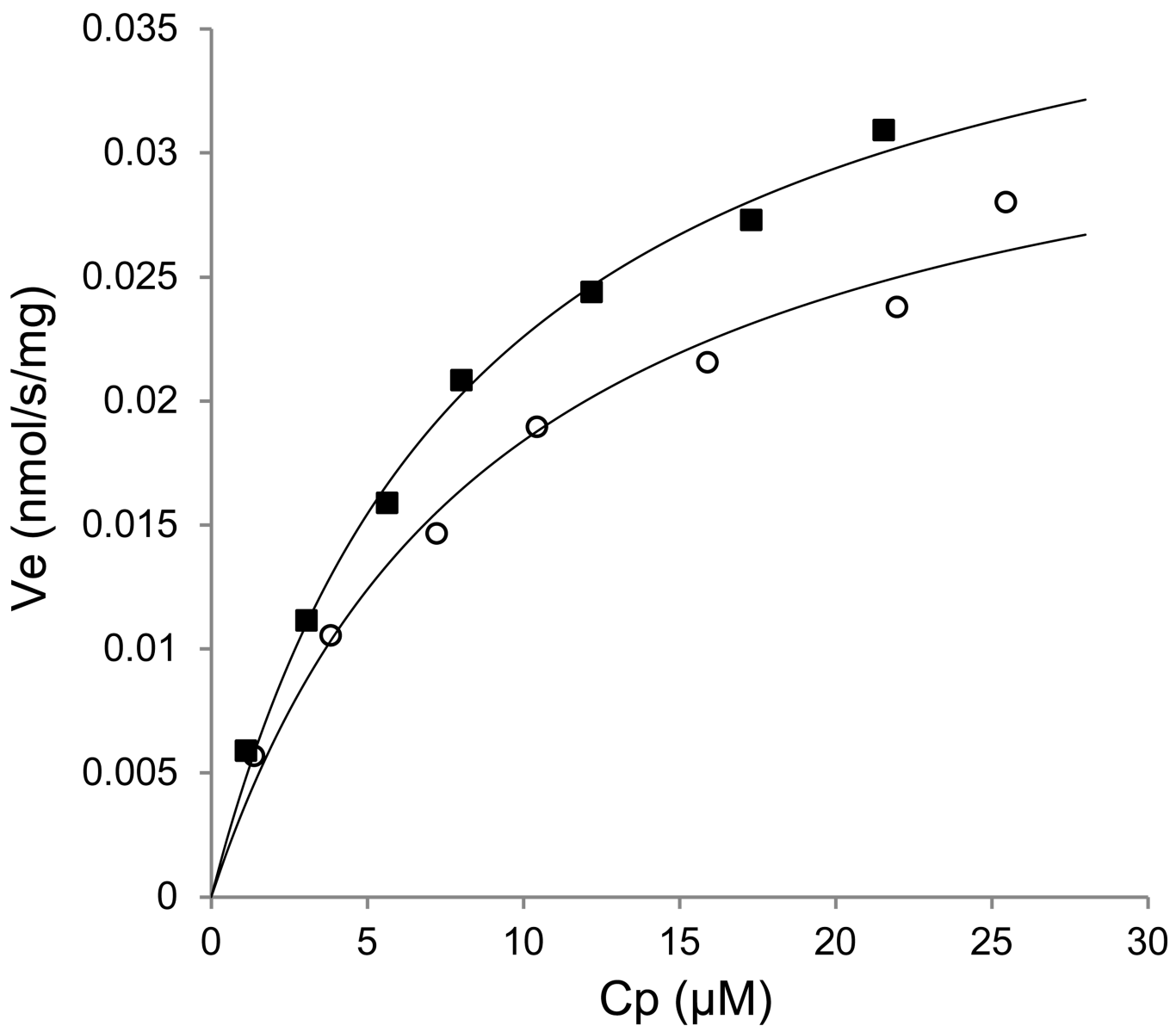
|            |                           |
|------------|---------------------------|
| <b>PCR</b> | polymerase chain reaction |
| <b>MD</b>  | molecular dynamics        |

## REFERENCES

1. Saier MH Jr, Paulsen IT, Sliwinski MK, Pao SS, Skurray RA, Nikaido H. Evolutionary origins of multidrug and drug-specific efflux pumps in bacteria. *FASEB J.* 1998; 12:265–274. [PubMed: 9506471]
2. Nikaido H. Multidrug efflux pumps of gram-negative bacteria. *J. Bacteriol.* 1996; 178:5853–5859. [PubMed: 8830678]
3. Ma D, Alberti M, Lynch C, Nikaido H, Hearst JE. The local repressor AcrR plays a modulating role in the regulation of *acrAB* genes of *Escherichia coli* by global stress signals. *Mol. Microbiol.* 1996; 19:101–112. [PubMed: 8821940]
4. Tsukagoshi N, Aono R. Entry into and release of solvents by *Escherichia coli* in an organic-aqueous two-liquid-phase system and substrate specificity of the AcrAB-TolC solvent-extruding pump. *J. Bacteriol.* 2000; 182:4803–4810. [PubMed: 10940021]
5. White DG, Goldman JD, Demple B, Levy SB. Role of the *acrAB* locus in organic solvent tolerance mediated by expression of *marA*, *soxS* or *robA* in *Escherichia coli*. *J. Bacteriol.* 1997; 179:6122–6126. [PubMed: 9324261]
6. Takatsuka Y, Chen C, Nikaido H. Mechanism of recognition of compounds of diverse structures by the multidrug efflux pump AcrB of *Escherichia coli*. *Proc. Natl. Acad. Sci. U. S. A.* 2010; 107:6559–6565. [PubMed: 20212112]
7. Nagano K, Nikaido H. Kinetic behavior of the major multidrug efflux pump AcrB of *Escherichia coli*. *Proc. Natl. Acad. Sci. U. S. A.* 2009; 106:5854–5858. [PubMed: 19307562]
8. Link AJ, Phillips D, Church GM. Methods for generating precise deletions and insertions in the genome of wild-type *Escherichia coli*: application to open reading frame characterization. *J. Bacteriol.* 1997; 179:6228–6237. [PubMed: 9335267]
9. Vargiu AV, Nikaido H. Multidrug binding properties of the AcrB efflux pump characterized by molecular dynamics simulations. *Proc. Natl. Acad. Sci. U. S. A.* 2012; 109:20637–20642. [PubMed: 23175790]
10. Trott O, Olson AJ. AutoDock Vina: improving the speed and accuracy of docking with a new scoring function, efficient optimization, and multithreading. *J Comput Chem.* 2010; 31:455–461. [PubMed: 19499576]
11. Sennhauser G, Amstutz P, Briand C, Storchenecker O, Grutter MG. Drug export pathway of multidrug exporter AcrB revealed by DARPin inhibitors. *PLoS Biol.* 2007; 5:e7. [PubMed: 17194213]
12. Humphrey W, Dalke A, Schulter K. VMD: Visual molecular dynamics. *J. Mol. Graph. Model.* 1996; 14:33–38.
13. Vargiu AV, Collu F, Schulz R, Pos KM, Zacharias M, Kleinekathofer U, Ruggerone P. Effect of the F610A mutation on substrate extrusion in the AcrB transporter: explanation and rationale by molecular dynamics simulations. *J. Am. Chem. Soc.* 2011; 133:10704–10707. [PubMed: 21707050]
14. Elkins CA, Nikaido H. Substrate specificity of the RND-type multidrug efflux pumps AcrB and AcrD of *Escherichia coli* is determined predominantly by two large periplasmic loops. *J. Bacteriol.* 2002; 184:6490–6498. [PubMed: 12426336]
15. Lomovskaya O, Warren MS, Lee A, Galazzo J, Fronko R, Lee M, Blais J, Cho D, Chamberland S, Renau T, Leger R, Hecker S, Watkins W, Hoshino K, Ishida H, Lee VJ. Identification and characterization of inhibitors of multidrug resistance efflux pumps in *Pseudomonas aeruginosa*: novel agents for combination therapy. *Antimicrob. Agents Chemother.* 2001; 45:105–116. [PubMed: 11120952]

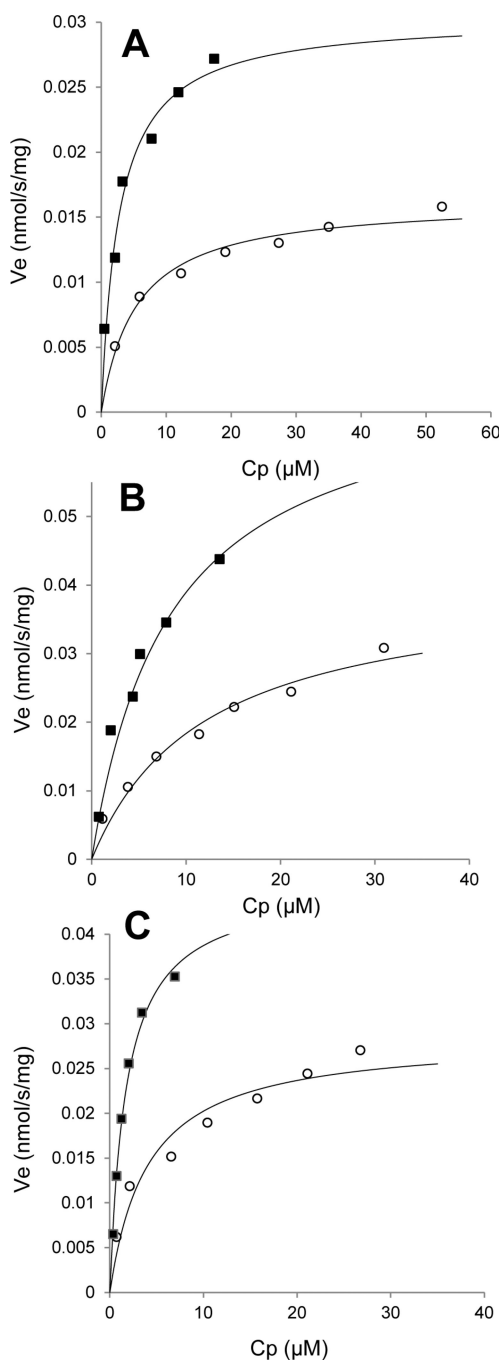
16. Lamers RP, Cavallari JF, Burrows LL. The efflux inhibitor phenylalanine-arginine beta-naphthylamide (PA $\beta$ N) permeabilizes the outer membrane of gram-negative bacteria. *PLoS One*. 2013; 8:e60666. [PubMed: 23544160]
17. Matsumoto Y, Hayama K, Sakakihara S, Nishino K, Noji H, Iino R, Yamaguchi A. Evaluation of multidrug efflux pump inhibitors by a new method using microfluidic channels. *PLoS One*. 2011; 6:e18547. [PubMed: 21533264]
18. Lomovskaya O, Bostian KA. Practical applications and feasibility of efflux pump inhibitors in the clinic--a vision for applied use. *Biochem. Pharmacol.* 2006; 71:910–918. [PubMed: 16427026]
19. Takatsuka Y, Nikaido H. Covalently linked trimer of the AcrB multidrug efflux pump provides support for the functional rotating mechanism. *J. Bacteriol.* 2009; 191:1729–1737. [PubMed: 19060146]
20. Barducci A, Bussi G, Parrinello M. Well-tempered metadynamics: A smoothly converging and tunable free-energy method. *Phys. Rev. Lett.* 2008; 100:020603. [PubMed: 18232845]
21. Biarnes X, Bongarzone S, Vargiu AV, Carloni P, Ruggerone P. Molecular motions in drug design: the coming age of the metadynamics method. *J. Comput. Aided Mol. Des.* 2011; 25:395–402. [PubMed: 21327922]
22. Laio A, Parrinello M. Escaping free-energy minima. *Proc. Natl. Acad. Sci. U. S. A.* 2002; 99:12562–12566. [PubMed: 12271136]
23. Vargiu AV, Ruggerone P, Magistrato A, Carloni P. Dissociation of minor groove binders from DNA: insights from metadynamics simulations. *Nucleic Acids Res.* 2008; 36:5910–5921. [PubMed: 18801848]
25. Shapiro AB, Ling V. Positively cooperative sites for drug transport by P-glycoprotein with distinct drug specificities. *Eur. J. Biochem.* 1997; 250:130–137. [PubMed: 9432000]
24. Shapiro AB, Fox K, Lam P, Ling V. Stimulation of P-glycoprotein-mediated drug transport by prazosin and progesterone. Evidence for a third drug-binding site. *Eur. J. Biochem.* 1999; 259:841–850. [PubMed: 10092872]
26. Lugo MR, Sharom FJ. Interaction of LDS-751 with P-glycoprotein and mapping of the location of the R drug binding site. *Biochemistry*. 2005; 44:643–655. [PubMed: 15641790]
27. Martin C, Berridge G, Higgins CF, Mistry P, Charlton P, Callaghan R. Communication between multiple drug binding sites on P-glycoprotein. *Mol. Pharmacol.* 2000; 58:624–632. [PubMed: 10953057]
28. Murakami S, Nakashima R, Yamashita E, Matsumoto T, Yamaguchi A. Crystal structures of a multidrug transporter reveal a functionally rotating mechanism. *Nature*. 2006; 443:173–179. [PubMed: 16915237]
29. Seeger MA, Schieffner A, Eicher T, Verrey F, Diederichs K, Pos KM. Structural asymmetry of AcrB trimer suggests a peristaltic pump mechanism. *Science*. 2006; 313:1295–1298. [PubMed: 16946072]
30. Husain F, Nikaido H. Substrate path in the AcrB multidrug efflux pump of *Escherichia coli*. *Mol. Microbiol.* 2010; 78:320–330. [PubMed: 20804453]
31. Yu EW, Aires JR, McDermott G, Nikaido H. A periplasmic drug-binding site of the AcrB multidrug efflux pump: a crystallographic and site-directed mutagenesis study. *J. Bacteriol.* 2005; 187:6804–6815. [PubMed: 16166543]
32. Drew D, Klepsch MM, Newstead S, Flraig R, De Gier JW, Iwata S, Beis K. The structure of the efflux pump AcrB in complex with bile acid. *Mol. Membr. Biol.* 2008; 25:677–682. [PubMed: 19023693]
33. Hung LW, Kim HB, Murakami S, Gupta G, Kim CY, Terwilliger TC. Crystal structure of AcrB complexed with linezolid at 3.5 Å resolution. *Journal of structural and functional genomics*. 2013; 14:71–75. [PubMed: 23673416]
34. Tornroth-Horsefield S, Gourdon P, Horsefield R, Brive L, Yamamoto N, Mori H, Snijder A, Neutze R. Crystal structure of AcrB in complex with a single transmembrane subunit reveals another twist. *Structure*. 2007; 15:1663–1673. [PubMed: 18073115]
35. Eicher T, Cha HJ, Seeger MA, Brandstatter L, El-Delik J, Bohnert JA, Kern WV, Verrey F, Grutter MG, Diederichs K, Pos KM. Transport of drugs by the multidrug transporter AcrB involves an

- access and a deep binding pocket that are separated by a switch-loop. Proc. Natl. Acad. Sci. U. S. A. 2012; 109:5687–5692. [PubMed: 22451937]
36. Nakashima R, Sakurai K, Yamasaki S, Nishino K, Yamaguchi A. Structures of the multidrug exporter AcrB reveal a proximal multisite drug-binding pocket. Nature. 2011; 480:565–569. [PubMed: 22121023]
37. Lim SP, Nikaido H. Kinetic parameters of efflux of penicillins by the multidrug efflux transporter AcrAB-TolC of *Escherichia coli*. Antimicrob. Agents Chemother. 2010; 54:1800–1806. [PubMed: 20160052]
38. Bemporad D, Luttmann C, Essex JW. Behaviour of small solutes and large drugs in a lipid bilayer from computer simulations. Biochim. Biophys. Acta. 2005; 1718:1–21. [PubMed: 16321606]
39. Plésiat P, Nikaido H. Outer membranes of gram-negative bacteria are permeable to steroid probes. Mol. Microbiol. 1992; 6:1323–1333. [PubMed: 1640833]
40. Nikaido H, Rosenberg EY. Porin channels in *Escherichia coli*: studies with liposomes reconstituted from purified proteins. J. Bacteriol. 1983; 153:241–252. [PubMed: 6294049]
41. Smirnova I, Kasho V, Kaback HR. Lactose permease and the alternating access mechanism. Biochemistry. 2011; 50:9684–9693. [PubMed: 21995338]
42. Ruggerone P, Murakami S, Pos KM, Vargiu AV. RND efflux pumps: structural information translated into function and inhibition mechanisms. Curr. Top. Med. Chem. 2013 in press.

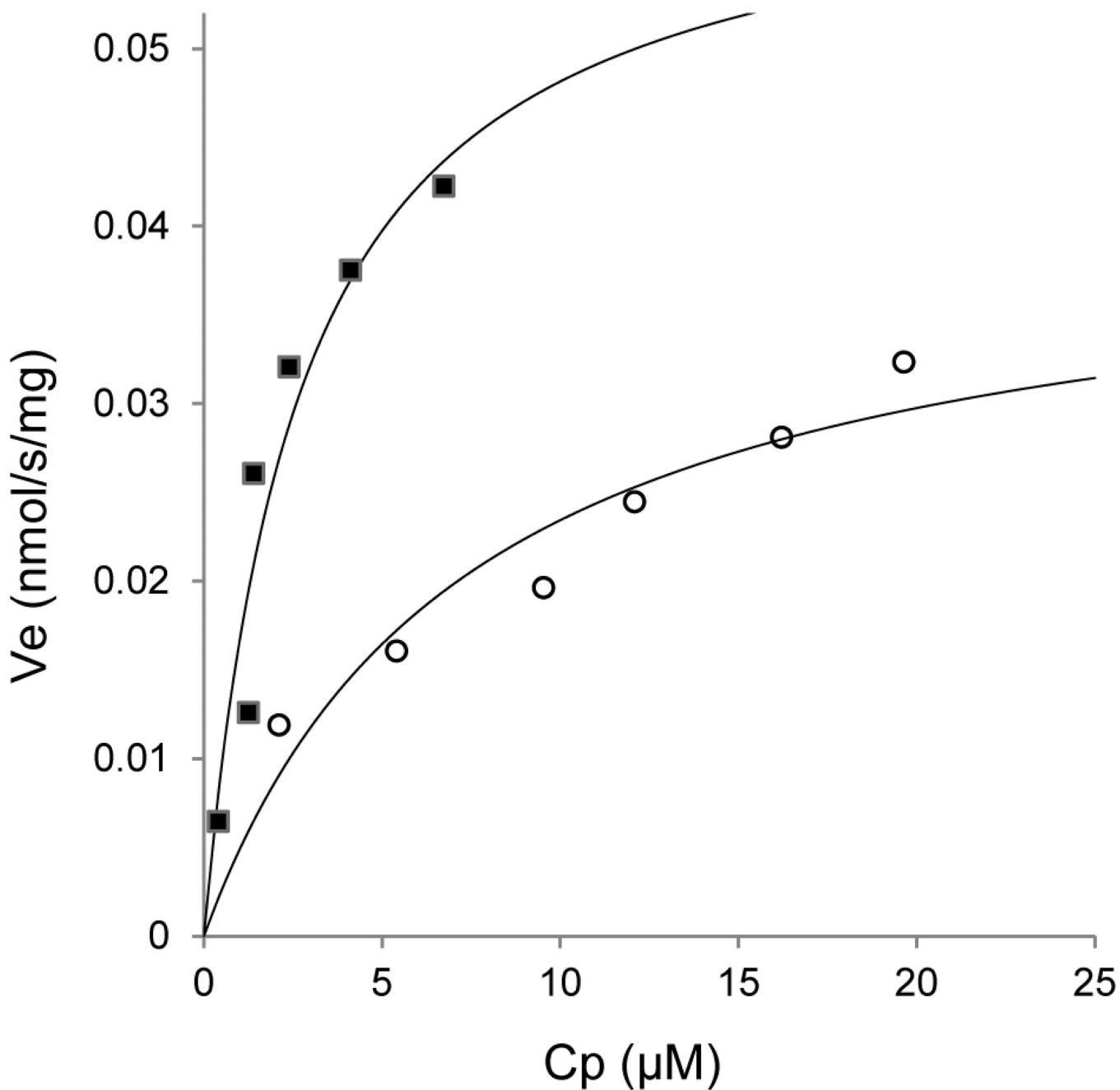


**Figure 1.**

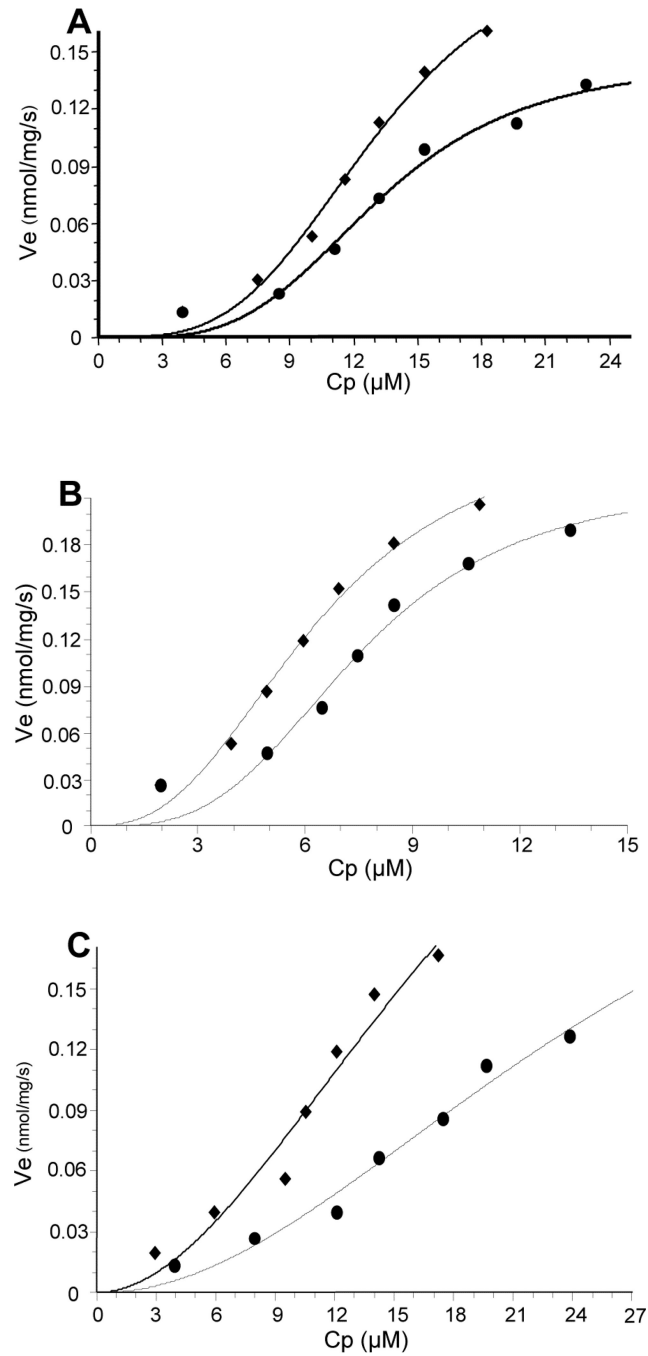
Chloramphenicol stimulates the efflux of nitrocefin. The efflux rate ( $V_e$ ) of nitrocefin is plotted against its periplasmic concentration ( $C_p$ ). Measurement was carried out in the absence (○) and presence (■) of 0.1 mM chloramphenicol. This experiment was repeated and gave essentially identical results.

**Figure 2.**

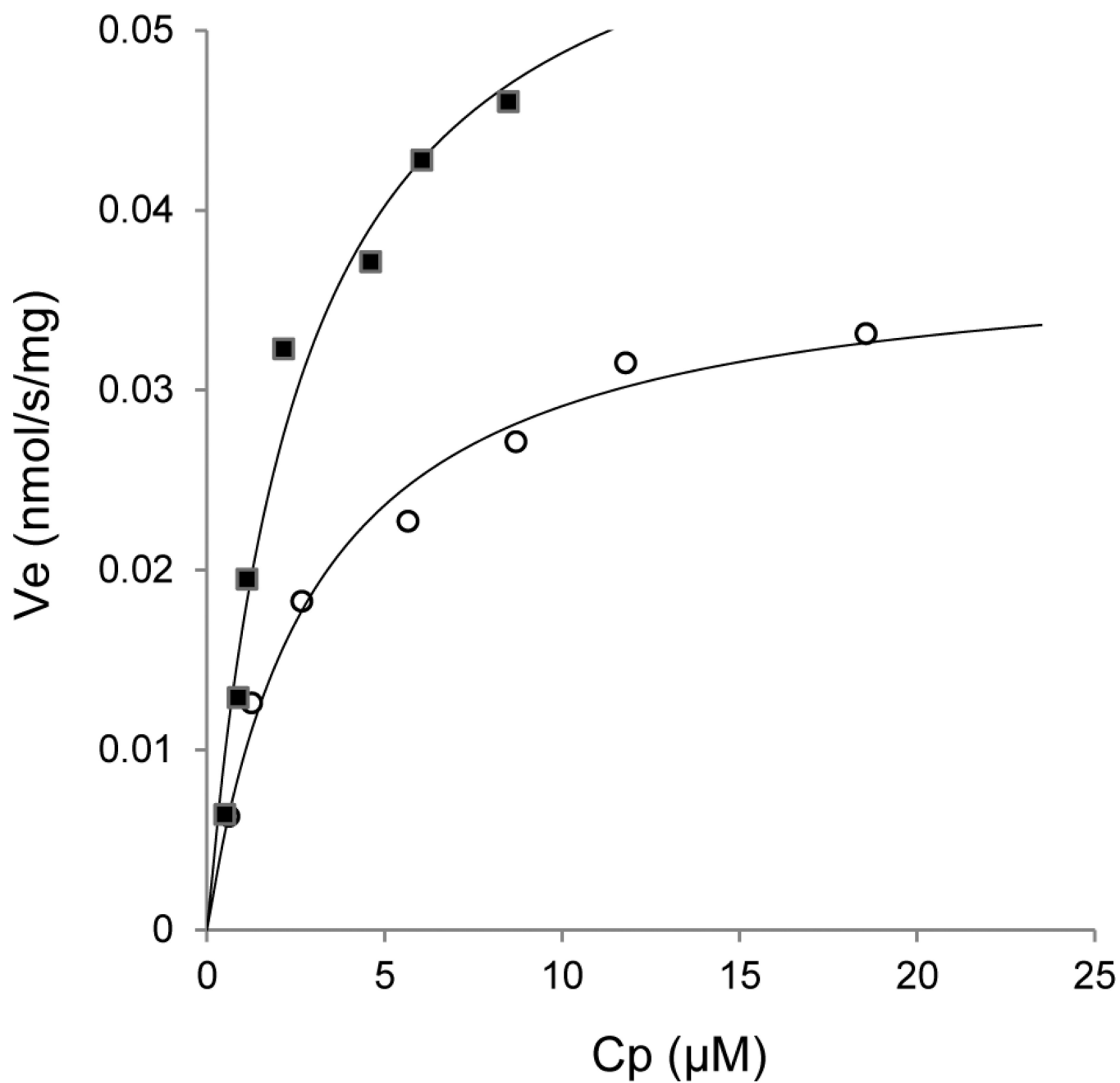
Stimulation of nitrocefin efflux by high concentrations (30 mM) of benzene (A) and cyclohexane (B), and 25 mM of cyclohexanone (C). Benzene and cyclohexane were added as a 1:1 (vol:vol) mixture with ethanol, and the same volume of 50% aqueous ethanol was added to the control. Cyclohexanone was similarly added as a 1:1 mixture with dimethylsulfoxide. As in Fig. 1, the efflux rates of nitrocefin ( $V_e$ ) are plotted against its periplasmic concentrations ( $C_p$ ). Measurement was carried out in the absence (○) and presence (■) of solvents. These experiments were repeated several times for each solvent, and reproducible results were obtained.



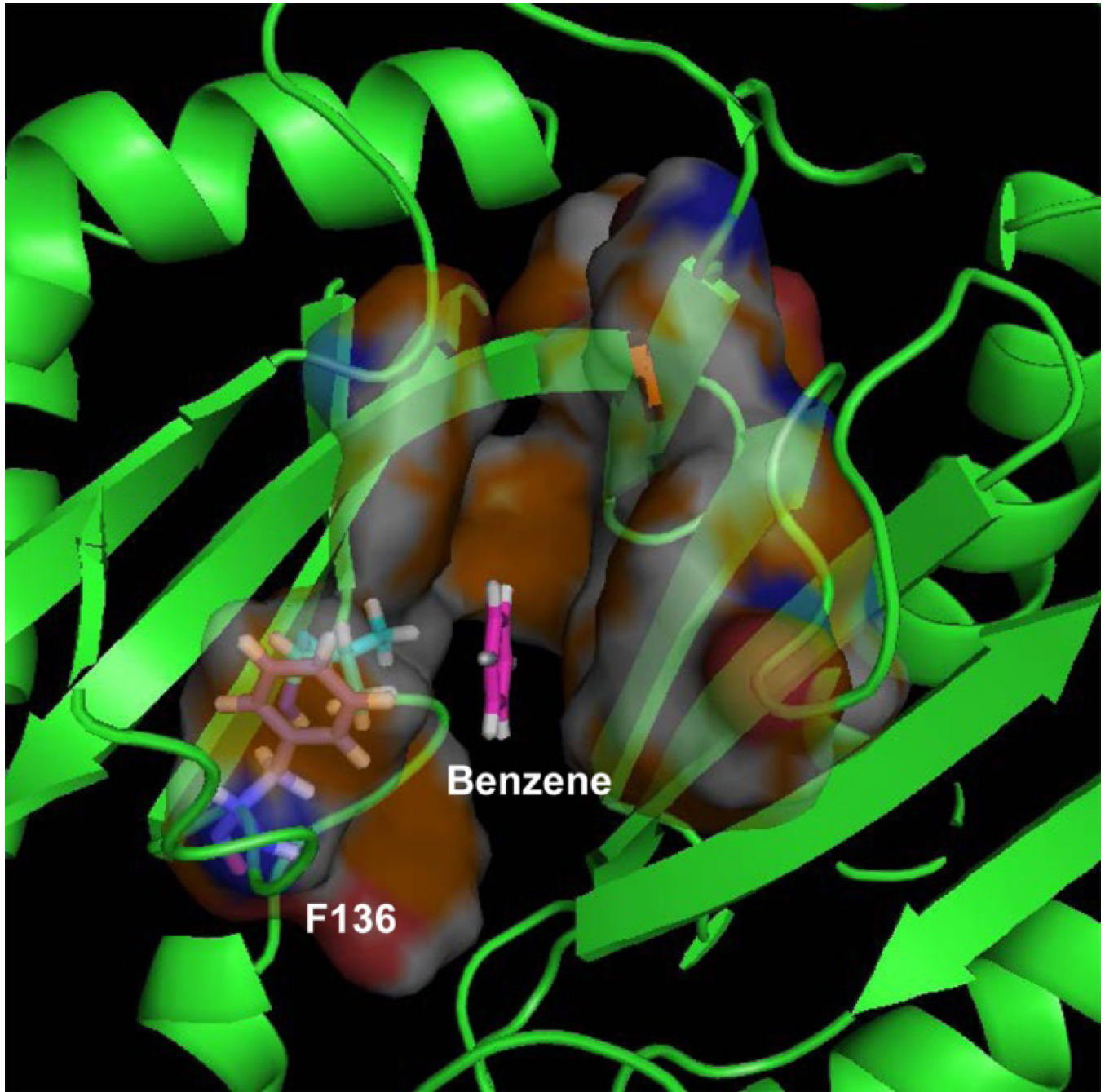
**Figure 3.**  
Stimulation of nitrocefin efflux by 0.1 mM Arg- $\beta$ -naphthylamide. As in Fig. 1,  $V_e$  of nitrocefin is plotted against its  $C_p$ . Measurement was carried out in the absence (○) and presence (■) of Arg- $\beta$ -naphthylamide. This experiment was repeated several times and reproducible data were obtained (see text).

**Figure 4.**

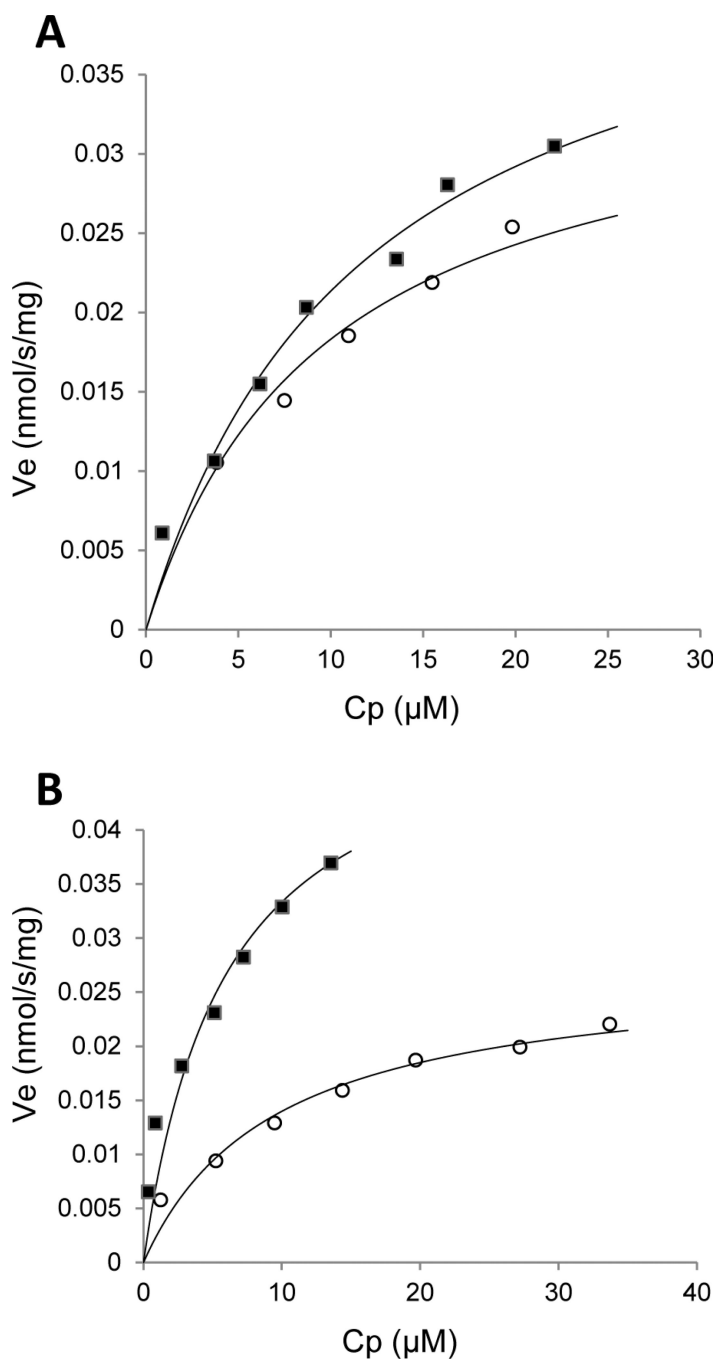
Stimulation of cefamandole efflux by 30 mM (A) and 0.1 mM (B) benzene, as well as 0.1 mM chloramphenicol (C). Measurement was carried out in the absence (■) and presence (◆) of stimulants. Each of these experiments was repeated several times, and reproducible results were obtained.

**Figure 5.**

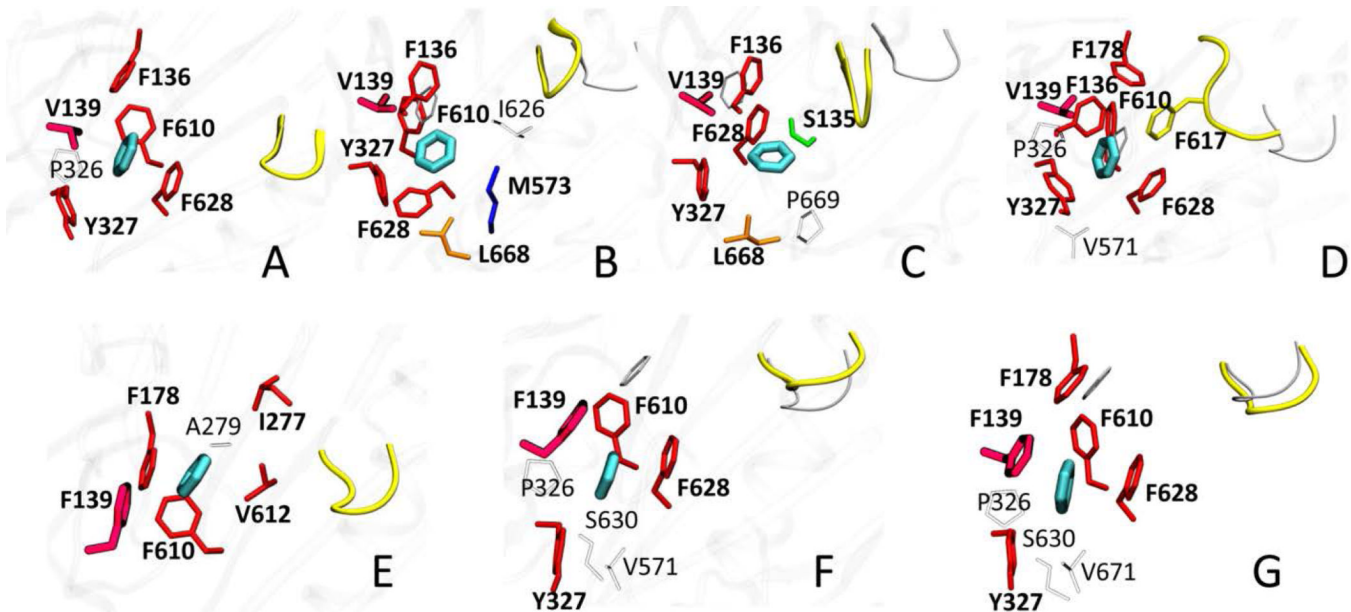
Stimulation of nitrocefin efflux occurs also in a covalently linked AcrB trimer. This figure shows a representative experiment in which nitrocefin efflux was measured in the absence (○) and presence (■) of 30 mM benzene.

**Figure 6.**

Docked position of benzene in the Binding Protomer of AcrB. This picture was produced by using the program PyMol.

**Figure 7.**

Stimulation of nitrocefin efflux by a low concentration (0.1 mM) of benzene. A. Cells producing the wild type AcrB. B. Cells producing the V139F mutant AcrB. These experiments were repeated several times, and similar results were obtained (see Table 1).

**Figure 8.**

Binding of benzene to the distal pocket of wt (A–D) and V139F variant (E–G) of AcrB. Sidechains of residues belonging to regions defined earlier<sup>9</sup> and within 3.5 Å from benzene are shown with solid sticks, with the following color code: distal pocket: red; cleft: orange; proximal pocket: green; distal/proximal pocket interface: blue; G-loop: yellow. V/F139 are shown with thicker sticks. Benzene is shown with cyan sticks, and the G-loop is highlighted in yellow for each pose. Docking conformations of benzene and of the G-loop are shown in grey in B–D and F–G. Residues not belonging to any relevant region are shown with transparent sticks.

A. Docking position in wt AcrB; B, C. Representative conformations, BNZ<sub>WT</sub> (1<sub>1</sub>) and BNZ<sub>WT</sub> (1<sub>2</sub>), sampled in simulation BNZ<sub>WT</sub> (1); D Representative conformation from BNZ<sub>WT</sub> (2); E. Docking position of BNZ in V139F AcrB; F–G. Representative conformations sampled in simulations BNZ<sub>V139F</sub> (1) and BNZ<sub>V139F</sub> (2).

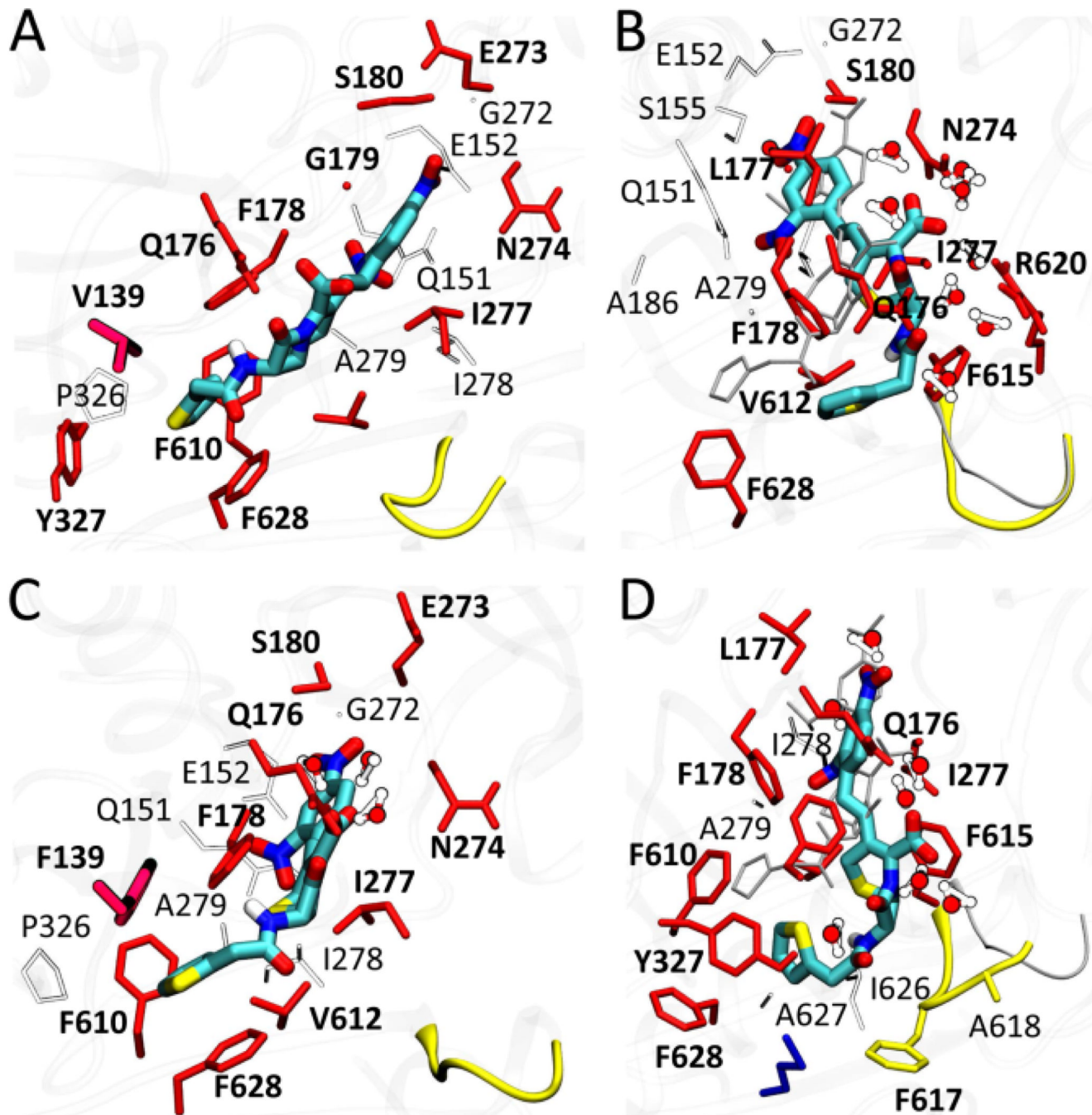


**Figure 9.**  
 Binding of nitrocefin to the distal pocket of wt (A–B) and V139F variant (C–D) of AcrB. A. Docking position in wt AcrB; B. Representative conformations sampled in NCF<sub>WT</sub>; C. Docking position in the V139F AcrB; D. Representative conformations sampled in NCF<sub>V139F</sub> (1).

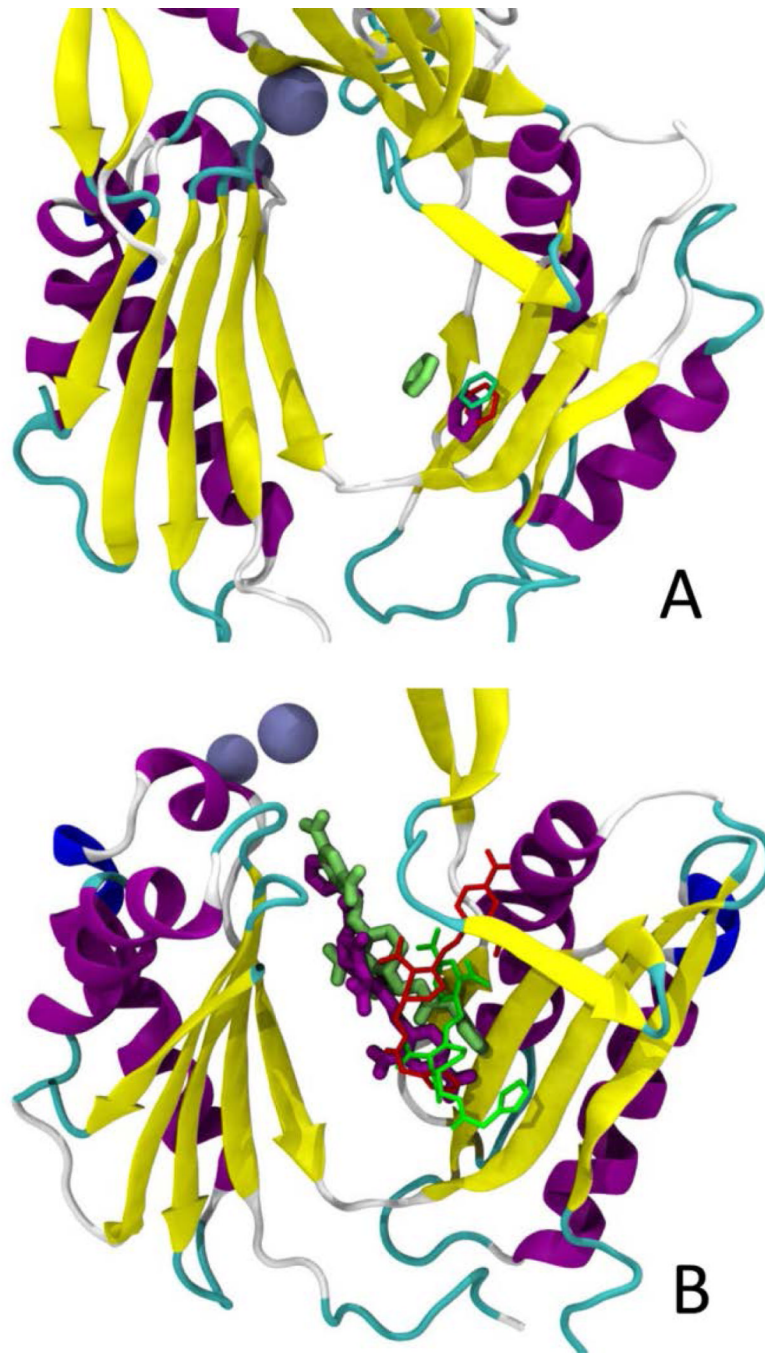


**Figure 10.**

Binding positions of benzene (A) and nitrocefén (B) in the bi- and tri-molecular complexes with AcrB. Thinner and thicker sticks represents the ligands in the bi-molecular and tri-molecular adducts respectively. Red and magenta indicate the wt complexes, while green and lime indicate the mutated ones. The protein is shown in cartoons and is colored according to the secondary structure. Residues Q124 and Y758 lining the gate to the central funnel are shown with ice blue beads.

$K_M$  and  $V_{max}$  of nitrocefin efflux.

Table 1

| Strains used | Without additive |                  | With Additive        |                |             |
|--------------|------------------|------------------|----------------------|----------------|-------------|
|              | $K_M$            | $V_{max}$        | Additive             | $K_M$          | $V_{max}$   |
| Wild type    | 10.3 ± 1.9 (9)   | 36.1 ± 9.8 (9)   | 0.1 mM Benzene       | 6.4 ± 0.1 (3)  | 41 ± 12 (3) |
|              |                  |                  | 0.1 mM Cyclohexane   | 7.0; 9.6       | 36; 26      |
|              |                  |                  | 0.1 mM Cyclohexanone | 10.4 ± 2.6 (4) | 47 ± 5 (4)  |
| V139F        | 10.2 ± 2.8 (10)  | 43.7 ± 14.6 (10) | 0.1 mM Benzene       | 4.1 ± 1.8 (3)  | 46 ± 15 (3) |
|              |                  |                  | 0.1 mM Cyclohexane   | 6.7 ± 2.6 (5)  | 48 ± 12 (5) |
|              |                  |                  | 0.1 mM Cyclohexanone | 5.1; 16.4      | 49; 72      |

$K_M$  and  $V_{max}$  values shown are average ± S.D., except in those cases where only two experiments were carried out, and in units of  $\mu\text{M}$  and  $\text{pmol/s/mg}$  (dry weight) cells, respectively. The numbers in parentheses show the number of independent experiments.

**Table 2**

Free energies and surface matching coefficients

| Compound <sup>a</sup>               | $\Delta G_b^b$   | Matching and Interactions |                        |             |            |             |            |         |                                |                              |      |
|-------------------------------------|------------------|---------------------------|------------------------|-------------|------------|-------------|------------|---------|--------------------------------|------------------------------|------|
|                                     | $\Delta G_{olv}$ | % of $\Delta G_b$         | Dist. Pkt <sup>c</sup> | Prox. Pkt   | G-loop     | Interface   | Ext. Cleft | BNZ/NCF | SM <sub>Tot</sub> <sup>d</sup> | SM <sub>L</sub> <sup>d</sup> | HB   |
| BNZ <sub>WT</sub> (1)               | -11.6±1.3        | -3.3 (28/59)              | -                      | -           | -0.4 (3/8) | -           | -          | 1.00    | 1.00                           | -                            | 1.07 |
| BNZ <sub>WT</sub> (1 <sub>2</sub> ) | -11.0±1.3        | -1.8 (28/59)              | -0.2 (1/3)             | -0.2 (2/5)  | -0.4 (3/9) | -0.7 (6/17) | -          | 0.96    | 0.98                           | -                            | -    |
| BNZ <sub>WT</sub> (2)               | -11.9±1.3        | -3.3 (27/58)              | -                      | -           | -          | -0.3 (2/6)  | -          | 1.00    | 1.00                           | -                            | 0.76 |
| BNZ <sub>V139F</sub> (1)            | -12.3±1.5        | -3.4 (27/56)              | -                      | -           | -          | -           | -          | 1.00    | 1.00                           | -                            | 1.46 |
| BNZ <sub>V139F</sub> (2)            | -12.5±1.2        | -3.2 (24/55)              | -                      | -           | -          | -           | -          | 0.87    | 0.93                           | -                            | 0.57 |
| NCF <sub>WT</sub>                   | -38.9±3.8        | -17.4 (44/68)             | -1.2 (3/4)             | -           | -1.0 (2/3) | -           | -          | 0.62    | 0.78                           | -                            | 0.61 |
| NCF <sub>V139F</sub>                | -42.0±3.8        | -14.1 (33/54)             | -                      | -           | -          | -           | -          | 0.49    | 0.63                           | -                            | 0.87 |
| NCF-BNZ <sub>WT</sub> (1, NCF)      | -34.2±3.7        | -11.2 (32/53)             | -                      | -2.8 (8/13) | -          | -           | -0.6 (2)   | n.c.    | n.c.                           | n.c.                         | n.c. |
| NCF-BNZ <sub>WT</sub> (1, BNZ)      | -12.2±1.5        | -2.6 (21/45)              | -                      | -0.3 (2/5)  | -0.3 (2/5) | -           | -0.4 (3)   | n.c.    | n.c.                           | n.c.                         | n.c. |
| NCF-BNZ <sub>WT</sub> (2, NCF)      | -32.9±4.4        | -15.7 (47/65)             | -                      | -           | -          | -           | -          | n.c.    | n.c.                           | n.c.                         | n.c. |
| NCF-BNZ <sub>WT</sub> (2, BNZ)      | -13.0±1.6        | -2.3 (18/48)              | -                      | -0.5 (3/9)  | -0.4 (3/8) | -0.4 (3/8)  | -          | n.c.    | n.c.                           | n.c.                         | n.c. |
| NCF-BNZ <sub>V139F</sub> (1, NCF)   | -41.2±3.4        | -18.2 (44/58)             | -                      | -2.3 (5/7)  | -          | -           | -          | n.c.    | n.c.                           | n.c.                         | n.c. |
| NCF-BNZ <sub>V139F</sub> (1, BNZ)   | -11.1±1.8        | -3.2 (28/60)              | -                      | -           | -0.5 (4/9) | -           | -          | n.c.    | n.c.                           | n.c.                         | n.c. |
| NCF-BNZ <sub>V139F</sub> (2, NCF)   | -41.1±2.8        | -18.0 (42/64)             | -                      | -           | -          | -           | -          | n.c.    | n.c.                           | n.c.                         | n.c. |
| NCF-BNZ <sub>V139F</sub> (2, BNZ)   | -12.4±1.2        | -3.3 (26/56)              | -                      | -           | -0.2 (1/3) | -           | -          | n.c.    | n.c.                           | n.c.                         | n.c. |

Numbers 1 and 2 in parenthesis refer to the simulation number thereon, with BNZ<sub>WT</sub> (11) and BNZ<sub>WT</sub> (12) indicating the two clusters of conformations found in the simulation of BNZ<sub>WT</sub> (1). The numbers in parentheses after the values of the contributions to  $\Delta G_{olv}$  from different regions indicate the percentages over the total free energy of binding (before slash) and the fraction of the total residues' contribution (after slash). n.c.: not calculated.

<sup>a</sup>The calculations for all compounds refer to the drugs bound to the distal pocket of the Binding protomer.

<sup>b</sup>The contribution of the configurational entropy of the solute has not been included (see SI). Concerning the contributions of different regions to  $\Delta G_b$ , only those larger than 2% are listed.